*atoms*

MDPI

*Article*

# Natural and Unnatural Parity Resonance States in the Positron-Hydrogen System with Screened Coulomb Interactions

**Ye Ning [1], Zong-Chao Yan [1] and Yew Kam Ho [2,*]**

Received: 22 November 2015; Accepted: 22 December 2015; Published: 26 December 2015
Academic Editors: Chi Yu Hu and Anand K. Bhatia

1 Department of Physics, University of New Brunswick, Fredericton NB E3B 5A3, Canada; ye.ning@unb.ca; zyan@unb.ca
2 Institute of Atomic and Molecular Sciences, Academia Sinica, Taipei 10617, Taiwan
* Correspondence: ykho@pub.iams.sinica.edu.tw; Tel.: +886-2-2366-8204; Fax: +886-2-2362-0200

**Abstract:** In the present work, we report calculations of resonances in the positron-hydrogen system interacting with screened Coulomb potentials using the method of complex scaling together with employing correlated Hylleraas wave functions. Resonances with natural and unnatural parities are investigated. For the natural parity case, resonance parameters (energy and width) for D-wave resonance states with even parity lying below various positronium and hydrogen thresholds up to the H(N = 4) level are determined. For the unnatural parity case, results for P-even and D-odd resonance states with various screened Coulomb interaction strengths are located below different lower-lying Ps and H thresholds.

**Keywords:** positron hydrogen; resonances; complex scaling; screened Coulomb potentials; Hylleraas functions; Debye plasmas

## 1. Introduction

Resonances in positron-hydrogen scattering were predicted by Mittleman [1], as they would exist below the $N = 2$ excited hydrogen threshold, a result of a dipole potential due to the $2s$-$2p$ degeneracy of the hydrogen atom, in a manner similar to that of the counter-part in electron-hydrogen scattering. Later, in a conclusive calculation using the complex scaling method and correlated Hylleraas wave functions in parametric form, Doolen *et al.* reported the lowest $S$-wave resonance lying below the H($N = 2$) threshold [2]. Since then, there have been considerable research activities on theoretical calculations of resonances in the positron hydrogen scattering (Refs. [3–13] and references therein). For resonances in positron atom scattering with the target other than the hydrogen atom, considerable theoretical activities have also been reported in the literature (Refs. [14–21], and references therein). The theoretical studies in atomic resonances involving positrons have been summarized in review articles throughout the years [22–26]. In a related development, atomic processes in plasmas have also attracted considerable attention (Ref. [27–36]). For weakly coupled plasmas such as Debye plasmas, the electronic interactions between charges are modeled with a screened Coulomb potential (SCP). Resonances in electron-atom scattering with SCP have been investigated in recent years [37–43]. Studies of positron-hydrogen scattering in plasmas such as the positronium formation cross sections have been reported [44–46]. Investigations on resonances in positron hydrogen resonances with SCP are relatively scarce, but it has started to attract attention [47–50]. Our present work represents one of such studies. Earlier, $S$-wave [47–49] and $P$-wave [49] resonances (with natural parities) in positron-hydrogen scattering with SCP were calculated. A state with parity of $(-1)^L$ is defined as a natural parity state, with $L$ being the total angular momentum of the system, and parity with value of +1 or $-1$ are called even or odd, respectively. A state with parity of $(-1)^{L+1}$ is called unnatural parity state. In the present work, we report a calculation on $D$-wave resonances with natural parity in $e^+$-H scattering with SCP. In addition, we have also investigated resonances with unnatural parities (the $P$-even and $D$-odd) resonance states with SCP for the first time, to the best of our knowledge. For pure Coulomb cases, resonances with unnatural parities in $e^+$-H system were reported in recent calculations [9–13]. Atomic units are used throughout in the present work.

## 2. Theory

Consider a three-body Coulomb system formed by an electron, a positron, and a proton, where the proton is assumed to be infinitely heavy, the non-relativistic Hamiltonian describing the unscreened positron-hydrogen system can be expressed as

$$H = T + V, \tag{1}$$

where

$$T = -\frac{1}{2}\nabla_1^2 - \frac{1}{2}\nabla_2^2 \tag{2}$$

is the kinetic energy operator, and

$$V = -\frac{1}{r_1} + \frac{1}{r_2} - \frac{1}{r_{12}}, \tag{3}$$

is the potential energy operator. In the above, the indices 1 and 2 refer, respectively, to the electron and the positron, $r_1$ and $r_2$ are their relative distance coordinates, measured from the nucleus of the hydrogen atom, and $r_{12}$ denotes the distance between the positron and electron. Recently, there has been considerable interest to investigate properties in atomic systems when the Coulomb interaction between charges is replaced by SCP. An example is when an atomic system is embedded in weakly coupled plasmas, such as Debye plasma modeled by a screening factor, the interaction potential between two charges $q_{\rm i}$ and $q_{\rm j}$, separated by a distance $r_{\rm ij}$, becomes

$$V\left(r_{\rm ij}\right) \;=\; q_{\rm i}\, q_{\rm j} \exp\left(-r_{\rm ij}/D\right)/r_{\rm ij}, \tag{4}$$

with $D$ being called the Debye length. Appling Equation (4) to Equation (3) results in

$$V = -\frac{1}{r_1}\exp\left(-\frac{r_1}{D}\right) + \frac{1}{r_2}\exp\left(-\frac{r_2}{D}\right) - \frac{1}{r_{12}}\exp\left(-\frac{r_{12}}{D}\right). \tag{5}$$

In the complex scaling method, under the complex transformation of the coordinates

$$r \rightarrow re^{i\theta}, \tag{6}$$

the Hamiltonian Equation (1) becomes complex

$$\hat{H}(\theta) = Te^{-2i\theta} + V_1, \tag{7}$$

with

$$V_1 = \left(-\frac{\exp\left(-r_1 e^{i\theta}/D\right)}{r_1} + \frac{\exp\left(-r_2 e^{i\theta}/D\right)}{r_2} - \frac{\exp\left(-r_{12} e^{i\theta}/D\right)}{r_{12}}\right) e^{-i\theta}. \tag{8}$$

Since the factor $r_{12}$ appearing in Equation (8) is a dynamical variable in the Hamiltonian, calculations of potential matrix elements require some efforts. In the present calculation, the complex-scaled SCP is approximated by using the Taylor series expansion

$$\exp\left(-re^{i\theta}/D\right) \approx \sum_{n=0}^{N} \frac{1}{n!}\left(-re^{i\theta}/D\right)^n. \tag{9}$$

A truncation for the above expansion to $N$, with a value ranging from 18 to 20 (*i.e.*, the order for $1/D$ increases up to the power of 17 to 19), is used throughout our work, as the smallest value for $D$ is restricted to 25 a.u. ($1/D < 0.04$). After some computational trails we believe that keeping the lowest 19 terms of the Taylor series (even they are in alternate "+" and "–" signs) in the expansion would be quite accurate for the problems investigated here. Another reason for keeping $1/D$ relatively small is that in the present work we concentrate on the Feshbach resonances (those lying below the respective two-body thresholds). As the screening strength $1/D$ increases, the Feshbach resonances may cross the thresholds to become shape resonances, and may even interact with other resonances, and as such, it would take more effort to analyze our results. For some limited cases (see details later in the text), we have examined the behaviors of resonances near the thresholds, but for the most part we use relatively small $1/D$ values to examine Feshbach resonances in our present work.

The calculations of the matrix elements are the same as those in Ref. [51]. After the expectation values of $r_{ij}$, $< r_{ij}{}^{n} >$, are calculated, they are then multiplied with respective scaling factor $e^{in\theta}/D^{n}$. The overall matrix elements for $H(\theta)$ can be determined by summing up all the contributing factors. The generalized complex eigenvalue problem for Hylleraas-type basis is then solved, in a matrix form, with

$$HC = ENC, \tag{10}$$

with

$$H_{ij} = \left\langle \psi_i \left| H(\theta) \right| \psi_j \right\rangle \text{ and } N_{ij} = \left\langle \psi_i \middle| \psi_j \right\rangle, \tag{11}$$

where $E$ and $C$ represent the eigenvalues and eigenvectors respectively, and $\{\Psi_i\}$ is the basis set for electron and positron (see later in the text). The resonance poles are determined by finding out the position where the complex eigenvalues exhibit the most stabilized characters with respect to the changes of rotation angle $\theta$ and the non-linear parameters in the basis set, *i.e.*,

$$\left.\frac{|\partial E_{res}|}{\partial \theta}\right|_{\alpha=\alpha_{opt}} = \text{minimum}, \quad \left.\frac{|\partial E_{res}|}{\partial \alpha}\right|_{\theta=\theta_{opt}} = \text{minimum}\,, \tag{12}$$

where $\alpha$ stands for such a non-linear parameter. It has been shown that the stationary conditions are associated with the cusps in $\theta$-trajectories with $\alpha$ held fixed (or in $\alpha$-trajectories with $\theta$ fixed) [22]. Once the position of the resonance pole is determined, the resonance energy $E_{\mathrm{r}}$ and total width $\Gamma$ are given by the following relation

$$E_{res} = E_r - \frac{i\Gamma}{2}. \tag{13}$$

Next, we construct our basis set using Hylleraas coordinates

$$\chi_{ijk}\left(\alpha,\beta\right) = r_1^i r_2^j r_{12}^k e^{-\alpha r_1 - \beta r_2} y_{\ell_1\ell_2}^{LM}\left(\hat{r}_1,\hat{r}_2\right), \tag{14}$$

where $y_{\ell_1\ell_2}^{LM}$ is the vector coupled product of spherical harmonics for the electron and the positron forming an eigenstate of the total angular momentum $L$ squared and $L_z$

$$y_{l_1 l_2}^{LM}\left(\hat{r}_1,\hat{r}_2\right) = \sum_{m_1 m_2} \left\langle l_1 l_2 m_1 m_2 \left| LM \right.\right\rangle Y_{l_1 m_1}\left(\hat{r}_1\right) Y_{l_2 m_2}\left(\hat{r}_2\right). \tag{15}$$

The indices $i$, $j$, and $k$ in Equation (14) are integers satisfying the conditions $i \geqslant l_1$, $j \geqslant l_2$ (for some test cases we use $j \geqslant 0$), and $k \geqslant 0$. The size of basis set is determined by $i + j + k \leqslant \Omega$, with $\Omega$ being an input integer. The explicit form of the wave function can be written in the form

$$\Psi(\mathbf{r}_1,\mathbf{r}_2) = \sum_{ijk} a_{ijk} x_{ijk}\left(\alpha,\beta\right), \tag{16}$$

where $a_{ijk}$ are the linear expansion coefficients. The required integrals for calculating matrix elements are of the type

$$\int d\mathbf{r}_1 d\mathbf{r}_2 Y_{l_1 m_1}(\hat{r}_1) Y_{l_2 m_2}(\hat{r}_2) r_1^a r_2^b r_{12}^c \exp(-\alpha r_1 - \beta r_2) \quad (17)$$

which can be evaluated analytically [51].

## 3. Results and Discussion

In the present investigation, we present results for *P*-wave and *D*-wave resonances in positron-hydrogen scattering. In a sense, the present work on the *D*-wave resonances with natural parity is a continuation of our earlier work [49] in that results for *S*-wave and *P*-wave resonances in this positron-hydrogen system with SCP were reported. In the earlier work, those are for natural parity resonances that would appear in scattering with the hydrogen atom in its ground state. Here, we also present results for unnatural parity resonances such as the *P*-even and *D*-odd states in the $e^+$-H system, and such resonances would only exist in scattering of positron with hydrogen atom in its excited states [9]. In the present work, as similar to the natural parity states, we consider the cases when the pure Coulomb potentials are replaced by SCP. The notation used to describe a resonance reported here is similar to that used in earlier works, such as $A_T(nl\text{-}k)$ is used for describing a resonance state, where $A_T$ denotes the target atom that can be either hydrogen H or positronium Ps, $n$ is the principal quantum number of the threshold state of $A_T$ below which the resonance lies, $l$ is the angular momentum of the target atom (H or Ps), and $k$ is the order of appearance of this resonance lying below the threshold of $A_T$. In the following subsections, we present our results, respectively, for *D*-wave resonances with natural parity, *P*-wave resonances with unnatural parity, and *D*-wave resonances with unnatural parity.

### 3.1. D-Wave Resonances with Natural Parity

We use three groups of expansion sets (see Equation (14)) to represent the *D*-state wave functions with natural parity. Using the notation $(l_1, l_2)$, where $l_1$ and $l_2$ denote the electron and positron angular momentum, respectively, the groups for *D*-states are (2, 0), (1, 1), and (0, 2), coupled to form the total angular momentum of $L = 2$. For each group, after trial and error, we use $\Omega = 18$ to ensure sufficient convergence of the energy eigenvalues, which leads to 816, 969, and 1140 terms, respectively, and the total number of terms used for the *D*-wave resonances with natural parity is hence 816 + 969 + 1140 = 2925. In addition, for practical purposes, in the present work we try to limit the total expansion lengths for our basis functions not to exceed 3000. As for the *P*-even case (later in text), we stop at $\Omega = 22$ with $N = 1771$ terms.

Next we show our results in Table 1. For the region below the H($N$ = 2) threshold we have calculated one resonance state (see Figure 1a,b). Figure 1a shows the changes in energy for changing $\mu$, with $\mu = 1/D$ representing the strength of screening effect. Figure 1b shows the changes for the corresponding $\Gamma/2$ when $\mu$ is changed. In Figure 1a we also show the energy level of the parent state, the 2$p$ state of the hydrogen atom in screening environments. For the region below the Ps($N$ = 2) threshold we show results for two members of resonances (see Figure 2a,b). Similarly, Figure 2a shows the changes in energies for the resonance states as well as for the parent Ps($N$ = 2) state when $\mu$ is changed, and Figure 2b shows the changes in the corresponding $\Gamma/2$ for increasing $\mu$. For the region below the H($N$ = 3) threshold we show the results for two Feshbach type resonances and one shape resonance lying above the H($N$ = 3) threshold (see Figure 3a–c)). For the region below the H($N$ = 4) threshold, we report three lowest lying resonances (see Figure 4a,b). In a similar fashion, the parts (a) in these figures show energies of the resonance states and of the respective parent states, and the other parts (b) and (c) in the figures show the corresponding changes in $\Gamma/2$. For screened Coulomb interactions between charged particles, in general, the resonance energies are all shifted upward due to the screening having a stronger effect on the attractive potentials than on the repulsive potentials. As for most of Feshbach-type resonances, the resonance width $\Gamma$ will exhibit a decreasing trend as the screening strength, $\mu = 1/D$, is increased. Such phenomenon can be explained as follows. The autoionization of a Feshbach type resonance is a result of momentum transfer, as the positron is knocked out by the electron, via the nucleus of H, after the positron is trapped by the excited target H forming a quasi-bound (resonance) state. Under screening environments, the movements of particles would be slower, hence prolonging (increasing) the lifetime of the quasi-bound (resonance) state, leading to a decrease of the resonance width, a result of the uncertainty principle. This will explain the behaviors for most of the $D$-wave resonances listed in Table 1, excepted for the shape resonance lying above the H($N$ = 3) threshold. The decay of a shape resonance is usually through tunneling. Under screening environments, the shape resonance, lying above the parent state in the pure Coulomb case, will move away from the parent threshold when the screening strength is increased. As a result, the thickness of the potential barrier, through which the positron tunnels out, will be decreased, resulting in shorter tunneling lifetime, and leading to broadening of the resonance width, again a consequence of the uncertainty principle. As for the H(2d-1) state, the width shows an increasing trend when $\mu$ is increased. In Figure 1a, it is seen that the energy level for the H(2d-1) state, a Feshbach resonance in the pure Coulomb case, is very close to the threshold of its parent state, the H(2p) level, and as such, a part of the wave function would overlap and pass over the threshold, resulting in some tunneling effect, leading to an increase of resonance width when the screening strength $\mu$ is increased. When $\mu$ is increased further, it even becomes a shape resonance as its energy now lies above the threshold of the H($N$ = 2) state (see Table 1), and its width would be further increased.

**Table 1.** $D$-wave resonances with natural parity in positron-hydrogen scattering with various Debye lengths $D$. The threshold energies $E_T$ are associated with the excited $nl$ states of the parent (H or Ps) atom. The notation A(−B) denotes A × $10^{-B}$. Units are in a.u.

| | $D$ | $E_r$ (a.u.) | Γ/2 (a.u.) | $E_T$ | H or Ps State |
|---|---|---|---|---|---|
| H(2d-1) | ∞ | −0.1250332 | 4.781(−6) | −0.125 | H(2p) |
| | ∞ | −0.12504795 [a] | 7.0(−7) [a] | | |
| | ∞ | −0.125047 [b] | 1.6(−6) [b] | | |
| | 200 | −0.1200768 | 4.847(−6) | −0.120061 | |
| | 100 | −0.115221 | 5.636(−6) | −0.115245 | |
| | 80 | −0.1128364 | 6.481(−6) | −0.112881 | |
| | 60 | −0.1089288 | 8.862(−6) | −0.109006 | |
| | 55 | −0.1075296 | 1.0132(−5) | −0.107616 | |
| | 50 | −0.1058663 | 1.2060(−5) | −0.105963 | |
| | 45 | −0.1038578 | 1.6244(−5) | −0.103962 | |
| Ps(2d-1) | ∞ | −0.071965 | 8.4198(−5) | −0.0625 | Ps(2p) |
| | ∞ | −0.07196495 [a] | 8.42(−5) [a] | | |
| | ∞ | −0.071943 [b] | 8.35(−6) [b] | | |
| | 100 | −0.0621949 | 8.3738(−5) | −0.052981 | |
| | 50 | −0.0529684 | 8.1573(−5) | −0.043647 | |
| | 40 | −0.048588 | 7.9652(−5) | −0.04037 | |
| | 30 | −0.0416585 | 7.5121(−5) | −0.03439 | |
| | 25 | −0.0364629 | 7.0354(−5) | −0.029556 | |
| Ps(2d-2) | ∞ | −0.0644753 | 3.5391(−5) | −0.0625 | Ps(2p) |
| | ∞ | −0.064475256 [a] | 3.48(−5) [a] | −0.052981 | |
| | ∞ | −0.064470 [b] | 3.43(−5) [b] | | |
| | 100 | −0.0547611 | 3.4798(−5) | | |
| | 50 | −0.0457653 | 3.1925(−5) | −0.043647 | |
| | 40 | −0.041582 | 3.0033(−5) | −0.04037 | |
| H(3d-1) | ∞ | −0.0572622 | 2.3161(−4) | −0.0555555 | H(3d) |
| | ∞ | −0.0572625 [a] | 2.32(−4) [a] | | |
| | ∞ | −0.057245 [b] | 2.18(−4) [b] | | |
| | 100 | −0.0475678 | 2.2505(−4) | −0.0460615 | |
| | 50 | −0.0387025 | 1.9549(−4) | −0.0375151 | |
| | 40 | −0.0346464 | 1.6929(−4) | −0.0335731 | |
| | 30 | −0.0285223 | 1.3558(−4) | −0.0274683 | |

**Table 1.** *Cont.*

| | $D$ | $E_r$ (a.u.) | $\Gamma/2$ (a.u.) | $E_T$ | H or Ps State |
|---|---|---|---|---|---|
| H(3d-2) | ∞ | −0.0558526 | 4.9653(−5) | −0.0555555 | H(3d) |
| | ∞ | −0.055825 [a] | 3.75(−5) [a] | | |
| | ∞ | −0.055825 [b] | 3.94(−5) [b] | | |
| | 100 | −0.046236 | 4.8893(−5) | −0.0460615 | |
| H (3d-shape) | ∞ | −0.055537 | 1.0938(−4) | −0.0555555 | H(3d) |
| | ∞ | −0.055542 [b] | 5.81(−5) [b] | | |
| | 100 | −0.0459933 | 1.1978(−4) | −0.0460615 | |
| | 50 | −0.0374707 | 1.6170(−4) | −0.0375151 | |
| | 40 | −0.0336156 | 2.5161(−4) | −0.0335731 | |
| | 30 | −0.0278024 | 5.0496(−4) | −0.0274683 | |
| H(4d-1) | ∞ | −0.0378252 | 3.0243(−5) | −0.03125 | H(4d) |
| | ∞ | −0.0378252 [a] | 3.025(−5) [a] | | |
| | ∞ | −0.037689 [b] | 3.12(−5) [b] | | |
| | 100 | −0.0282273 | 2.9930(−5) | −0.0222278 | |
| | 50 | −0.0197682 | 2.6997(−5) | −0.0149401 | |
| | 40 | −0.0160542 | 2.4349(−5) | −0.0118705 | |
| | 30 | −0.0106871 | 1.8529(−5) | −0.0075338 | |
| H(4d-2) | ∞ | −0.0349288 | 3.6679(−5) | −0.03125 | H(4d) |
| | ∞ | −0.03492875 [a] | 3.67(−5) [a] | | |
| | ∞ | −0.034 689 [b] | 3.71(−5) [b] | | |
| | 100 | −0.0255062 | 3.5656(−5) | −0.0222278 | |
| | 50 | −0.0173876 | 3.1467(−5) | −0.0149401 | |
| | 40 | −0.0138584 | 2.8036(−5) | −0.0118705 | |
| | 30 | −0.0088013 | 2.1274(−5) | −0.0075338 | |
| H(4d-3) | ∞ | −0.0334566 | 2.4389(−5) | −0.03125 | H(4d) |
| | ∞ | −0.0334564 [a] | 2.44(−5) [a] | | |
| | ∞ | −0.033 342 [b] | 2.47(−5) [b] | | |
| | 100 | −0.0239507 | 2.3450(−5) | −0.0222278 | |
| | 50 | −0.0159279 | 1.7544(−5) | −0.0149401 | |

[a] Ref. [7]; [b] Ref. [13].

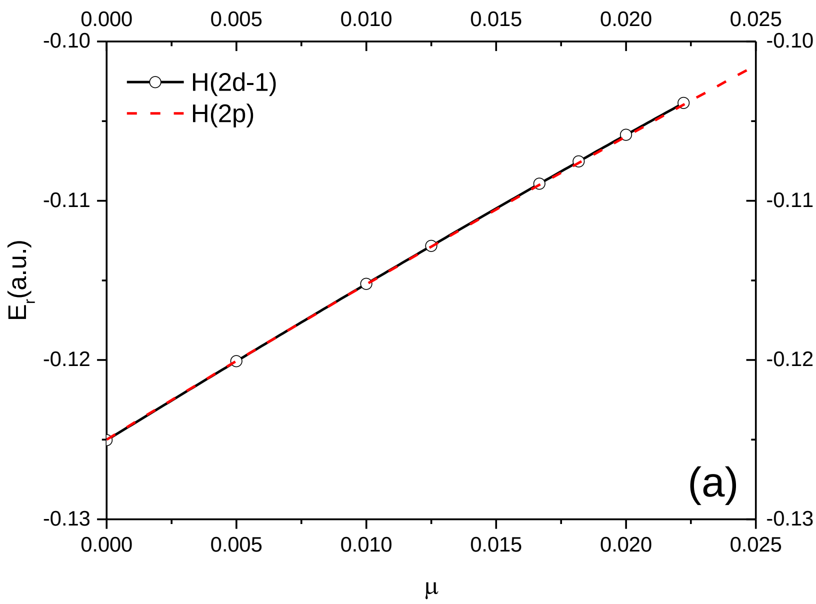


**Figure 1.** *Cont.*

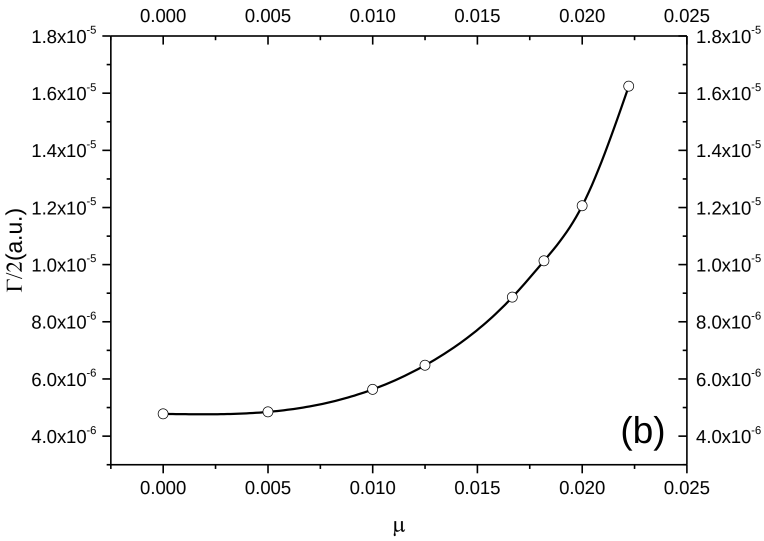


**Figure 1.** *D*-wave (**a**) resonance energy and (**b**) half-width for the H(2d-1) state as a function of $\mu = 1/D$.

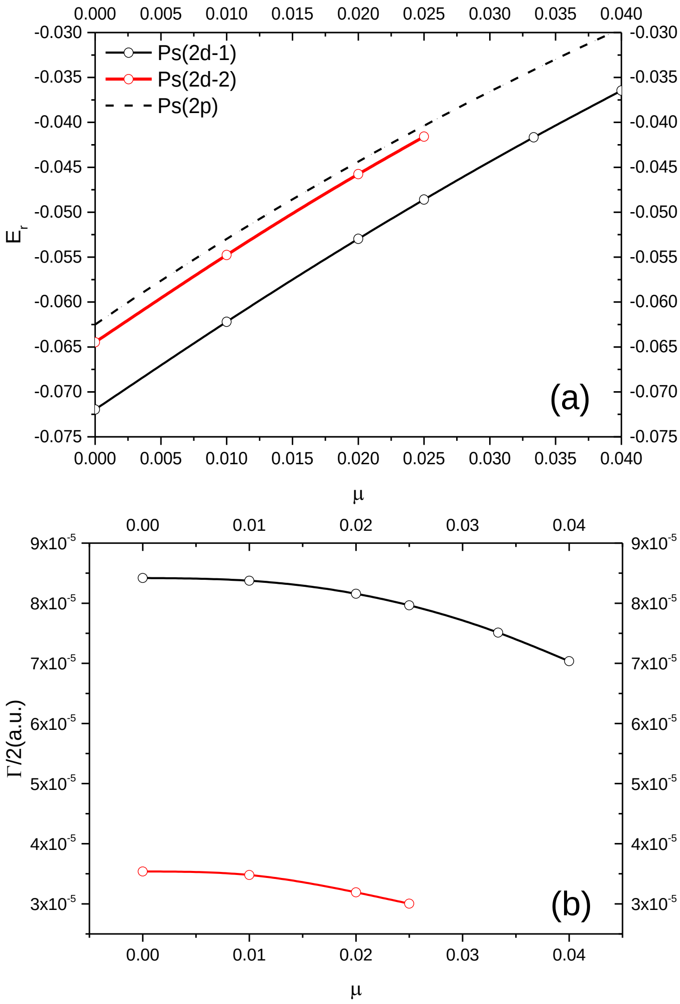


**Figure 2.** *D*-wave (**a**) resonance energy and (**b**) half-width for the Ps(2d-$k$) states with $k = 1$ and 2 as a function of $\mu = 1/D$.

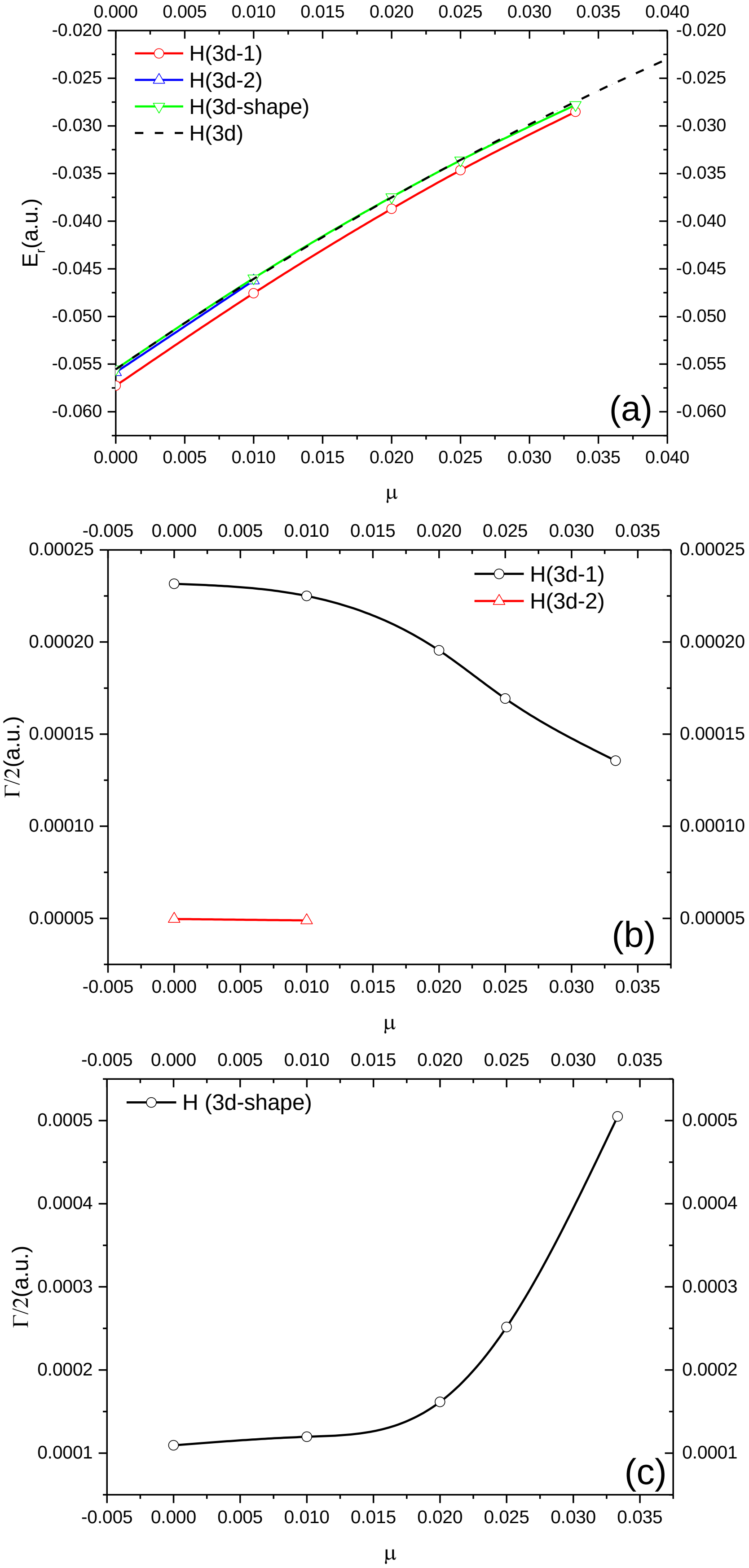


**Figure 3.** *D*-wave (**a**) resonance energy and (**b**) half-width for the H(3d-*k*) states with $k = 1$, 2, and (**c**) shape resonance, as a function of $\mu = 1/D$.

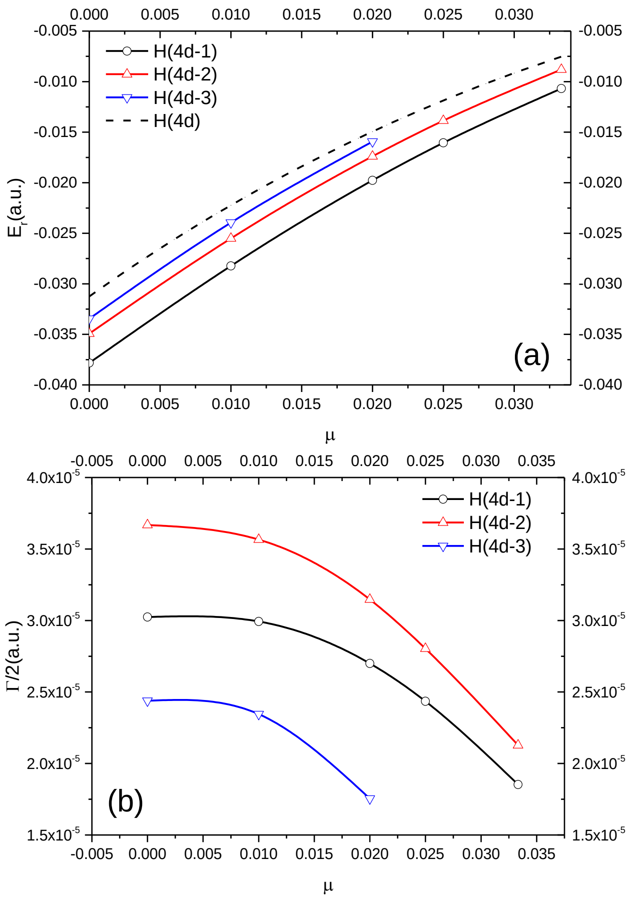


**Figure 4.** *D*-wave (**a**) resonance energy and (**b**) half-width for the H (4d-*k*) states with $k = 1, 2, 3$ as a function of $\mu = 1/D$.

## 3.2. P-Wave Resonances with Unnatural Parity

For this case, we use one group of expansion (see Equation (14)) to construct the wave functions, and in the notation $(l_1, l_2)$, it is (1, 1) coupled to form the total angular momentum state of $L = 1$. For this group, we use $\Omega = 22$, which leads to 1771 terms used for the *P*-wave resonances with unnatural parity. Such *P*-even resonances are denoted as $P^e$ states. We present our numerical results for these states in Table 2 and they are plotted in Figures 5–8. For the region below the Ps($N = 2$) threshold we have calculated one state, and Figure 5a shows the changes in resonance energy and the parent Ps(2*p*) state energy for changing $\mu$, and Figure 5b shows the changes in the corresponding $\Gamma/2$ when $\mu$ is changed. For the region below the H($N = 3$) threshold we show results for one resonance. Figure 6a,b are for, respectively, changing energies and changing $\Gamma/2$. For this resonance it is denoted as H(3p$^e$-1). Figure 7a,b are for, respectively, changing energies and changing $\Gamma/2$, for two resonances lying below the H($N = 4$) threshold. Under the screening influences, the states denoted as H(4p$^e$-1) and H (4p$^e$-2) show decreasing in width when the screening strength $\mu$ is increased. This can be explained in a similar way as those for the Feshbach resonances discussed above in Section 3.1. As for the Ps(2p$^e$-1) and H(3p$^e$-1) states, the widths show an increasing trend when $\mu$ is increased. In Figure 6a it is seen that the energy level for the H(3p$^e$-1) state is very close to the threshold of its parent state, the H(3p) level, and the tunneling effect from part of its wave packet would lead to increasing in width as the screening strength $\mu$ is increased. Such phenomenon is similar to that for the H(2d-1) state with natural parity, as discussed in Section 3.1. As for the Ps(2p$^e$-1) state, its width also shows an increasing trend when the screening strength is increased (see Figure 5b). An explanation for such a behavior is not so certain at present, as on one hand this state is of Feshbach type and we might expect that its width would show a decreasing trend for increasing $\mu$. But on the other hand, its resonance position is quite close to the parent threshold, and thus the tunneling effect may play a dominate role for this unnatural parity resonance. Nevertheless, the reported resonance parameters are quite accurate, and we hope that our results would stimulate further investigations on this system in order to shed light on such an intriguing phenomenon.

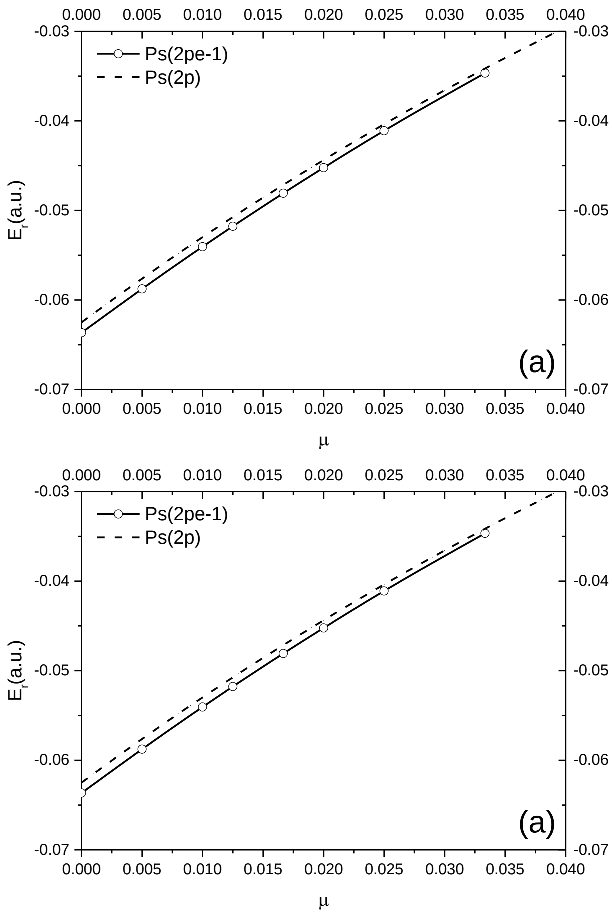


**Figure 5.** *P*-wave unnatural parity states: (**a**) resonance energy and (**b**) half-width for the Ps(2p$^e$-1) state as a function of $\mu = 1/D$.

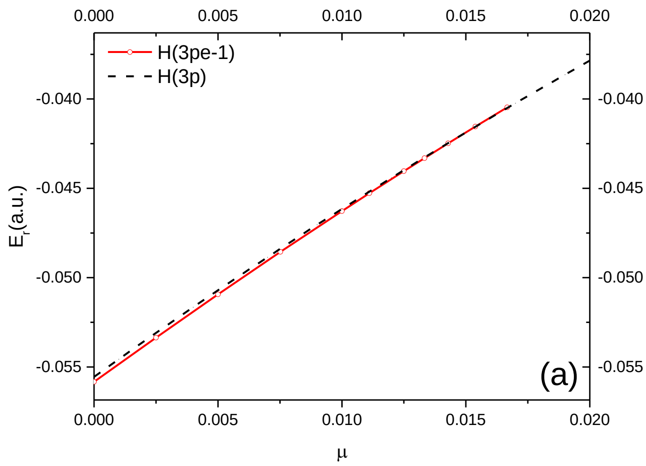


**Figure 6.** *Cont.*

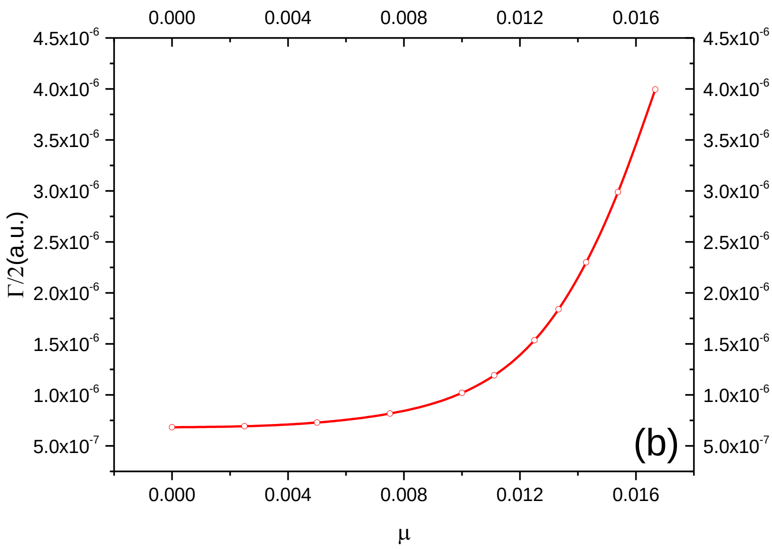


**Figure 6.** *P*-wave unnatural parity states: (**a**) resonance energy and (**b**) half-width for the H(3p$^e$-1) state as a function of $\mu = 1/D$.

**Table 2.** *P*-wave resonances with unnatural parity in the positron-hydrogen system with various Debye lengths *D*. The threshold energies $E_T$ are associated with the excited *np* states of the parent (H or Ps) atom. The notation A(−B) denotes. A × $10^{-B}$. Units are in a.u.

| | ***D*** | **$E_r$ (a.u.)** | **Γ/2 (a.u.)** | **$E_T$** | **H or Ps State** |
|---|---|---|---|---|---|
| Ps(2p$^e$-1) | ∞ | −0.0636595 | 2.0486(−7) | −0.0625 | Ps(2p) |
| | ∞ | −0.06366 [a] | 2.05(−6) [a] | | |
| | ∞ | −0.06366 [b] | 2.06(−7) [b] | | |
| | 200 | −0.0587580 | 2.0717(−7) | −0.057622 | |
| | 100 | −0.0540528 | 2.1353(−7) | −0.052981 | |
| | 80 | −0.0517734 | 2.1794(−7) | −0.050746 | |
| | 60 | −0.0480825 | 2.2669(−7) | −0.047141 | |
| | 50 | −0.0452267 | 2.3461(−7) | −0.044363 | |
| | 40 | −0.0411039 | 2.4891(−7) | −0.04034 | |
| | 30 | −0.0346595 | 2.8003(−7) | −0.03439 | |
| H(3p$^e$-1) | ∞ | −0.0558317 | 6.8305(−7) | −0.0555555 | H(3p) |
| | ∞ | −0.05583 [a] | 6.0(−7) [a] | | |
| | ∞ | −0.05583 [b] | 7.04(−7) [b] | | |
| | 200 | −0.0509363 | 7.2906(−7) | −0.0507082 | |
| | 100 | −0.0462736 | 1.0203(−6) | −0.046153 | |
| | 80 | −0.0440384 | 1.5356 (−6) | −0.0439795 | |
| | 60 | −0.0404682 | 3.9950(−6) | −0.0405044 | |
| | 50 | −0.0377501 | 1.4440(−5) | −0.037852 | |
| H(4p$^e$-1) | ∞ | −0.0355781 | 2.3006(−5) | −0.03125 | H(4p) |
| | ∞ | −0.03558 [a] | 2.3(−5) [a] | | |
| | ∞ | −0.03557 [b] | 2.30(−5) [b] | | |
| | 100 | −0.0261443 | 2.2093(−5) | −0.0222278 | |
| | 50 | −0.0179889 | 1.8826(−5) | −0.0149401 | |
| | 40 | −0.0144318 | 1.6415(−5) | −0.0118705 | |
| | 30 | −0.0093060 | 1.0714(−5) | −0.0075338 | |
| H(4p$^e$-2) | ∞ | −0.03214774 | 9.5498(−6) | −0.03125 | H(4p) |
| | ∞ | −0.03215 [a] | 9.5(−6) [a] | | |
| | ∞ | −0.03214 [b] | 1.25(−5) [b] | | |
| | 100 | −0.0228160 | 8.2815(−6) | −0.0222278 | |
| | 80 | −0.0207323 | 7.3668(−6) | −0.0203829 | |
| | 60 | −0.0175160 | 5.4189(−6) | −0.0174078 | |

[a] Ref. [9]; [b] Ref. [13].

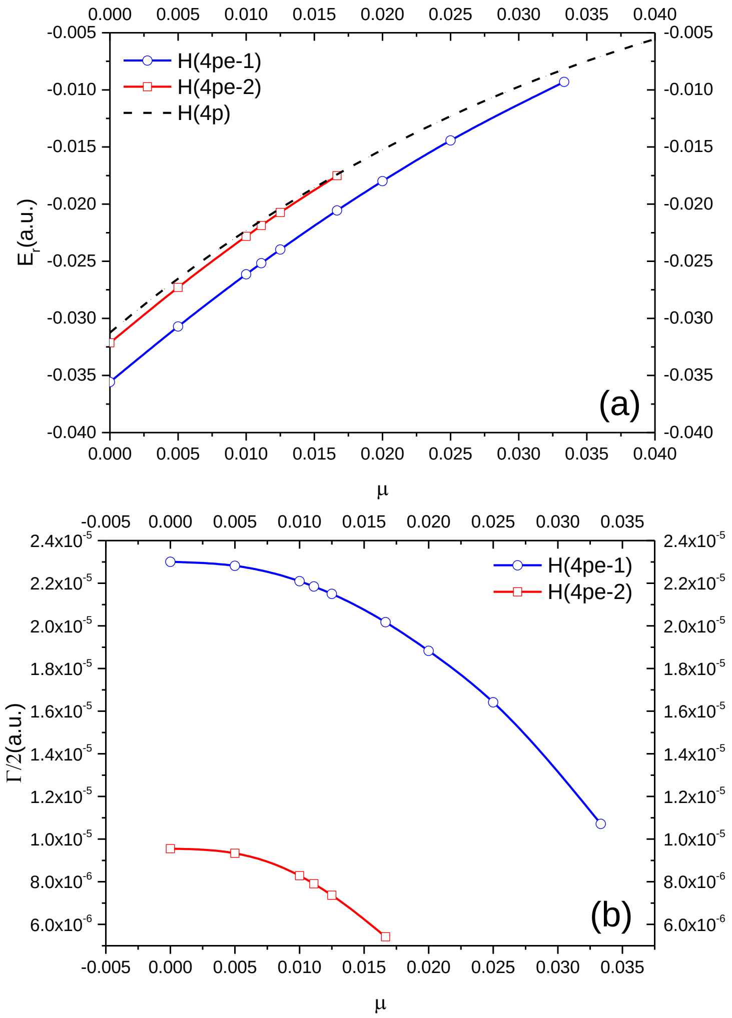


**Figure 7.** *P*-wave states with unnatural parity: (**a**) resonance energy and (**b**) half-width for the H($4p^e$-$k$) states with $k = 1, 2$ as a function of $\mu = 1/D$.

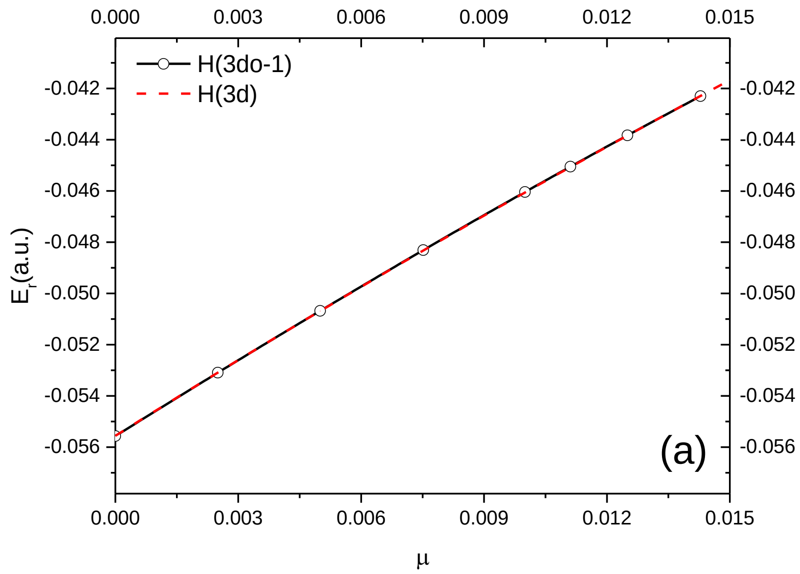


**Figure 8.** *Cont.*

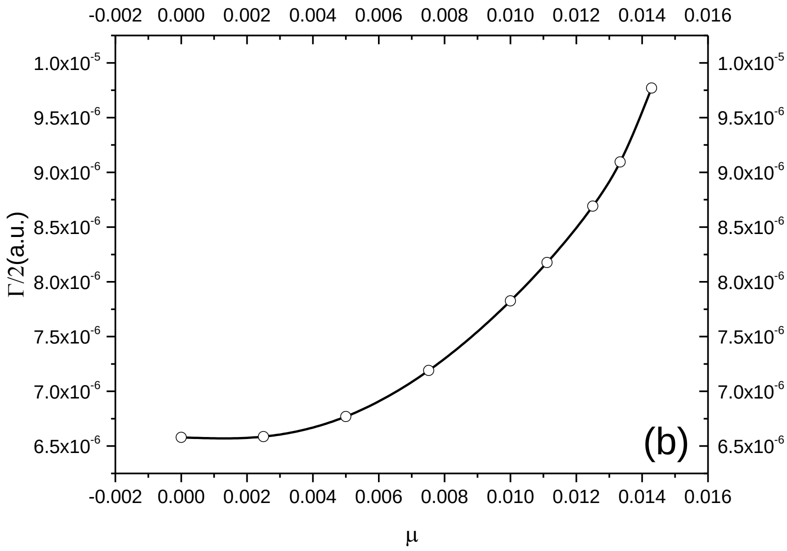


**Figure 8.** *D*-wave states with unnatural parity: (**a**) resonance energy and (**b**) half-width for the H(3d°-1) state, as a function of $\mu = 1/D$.

### *3.3. D-Wave Resonances with Unnatural Parity*

For *D*-wave resonance states with unnatural parity, we use two groups of expansion (see Equation (14)) to construct their wave functions. In the notation $(l_1, l_2)$ as described before, they are (2, 1) and (1, 2), coupled to form the total angular momentum $L = 2$ for such states. For each group, we use $\Omega = 21$, which leads to 1330 and 1540 terms, respectively, and the total number of terms used for the *D*-wave resonances with unnatural parity is hence 1330 + 1540 = 2870. We show our results in Table 3. For the region below the H($N = 3$) threshold we have calculated one state, denoted as H(3d°-1), and Figure 8a shows the changes in the resonance energy and in the energy of the parent H(3d) state for changing $\mu$, and Figure 8b shows the corresponding $\Gamma/2$ when $\mu$ is changed. For the region below the H($N = 4$) threshold we show results for four members of resonances. Figure 9a,b are for, respectively, changing energies and changing $\Gamma/2$, for the lowest-lying three members of resonances, denoted as H(4d°-1), H(4d°-2) and H(4d°-3). Figure 9a also shows the changes in the parent H(4d) state for changing $\mu$. Figure 10a,b are for, respectively, changing energies and changing $\Gamma/2$, for the H(4d°-4) state. Returning to the H(3d°-1) state which lies below the H($N = 3$) threshold, for screened Coulomb interactions between charged particles the energy for such a state lies very close to the threshold energy of its parent state (see Figure 8a). When the screening strength $\mu$ is increased the resonance width shows an increasing trend. This implies that a part of the resonance wave function exhibits some overlapping behavior with the threshold of the parent state, and hence the tunneling effect similar to a shape resonance would occur, leading to the increase of resonance width as $\mu$ is increased (see Figure 8b). As for the resonances below the H($N = 4$) threshold, the three lowest-lying members (see Figure 9a) all show a decreasing trend for increasing $\mu$. Such phenomenon is in line with the fact that they are Feshbach type resonances (see Section 3.1 for an explanation). Figure 10a shows the energy level for the fourth member below the H($N = 4$) threshold. As such a resonance state lies very close to the parent threshold, the phenomenon is very much similar to that of the H($N = 3$) state, and as part of the wave function exhibiting tunneling effect, it would lead to the increase in resonance width when the screening strength $\mu$ is increased. Lastly, it should be mentioned that we have not found any *D*-wave odd parity resonances below the positronium $N = 2$ threshold. This is consistent with our earlier findings [9], and also with other earlier results [20].

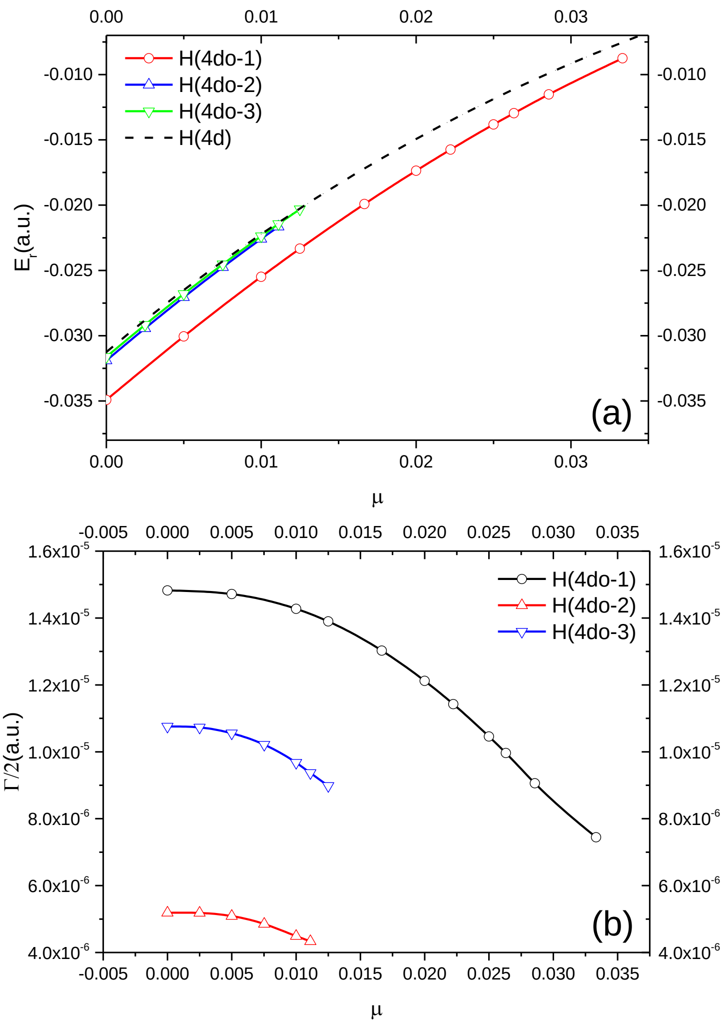


**Figure 9.** *D*-wave states with unnatural parity: (**a**) resonance energy and (**b**) half-width for the H(4d$^{\circ}$-$k$) states, with $k$ = 1, 2, 3 as a function of $\mu = 1/D$.

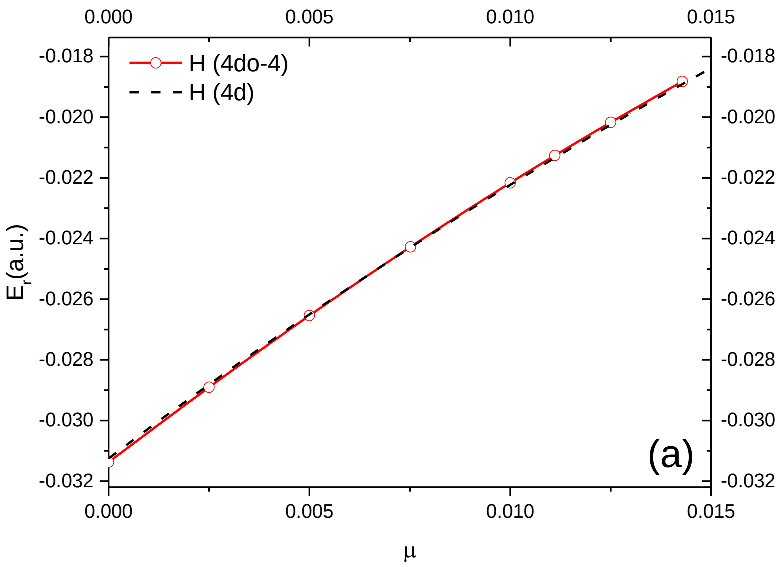


**Figure 10.** *Cont.*

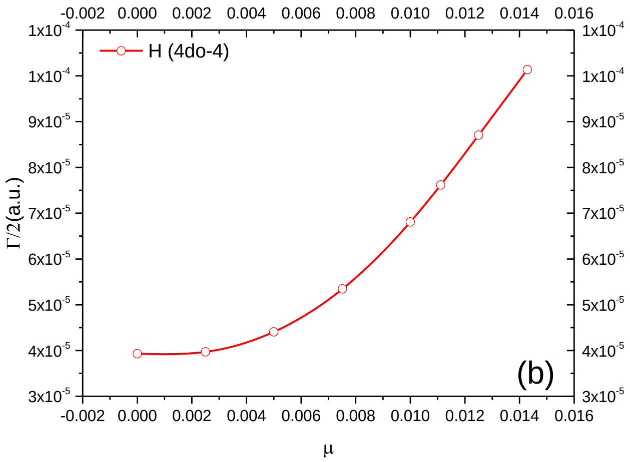


**Figure 10.** *D*-wave states with unnatural parity: (**a**) resonance energy and (**b**) half-width for the H(4d°-4) state as a function of $\mu = 1/D$.

**Table 3.** *D*-wave resonances with unnatural parity in the positron-hydrogen system with various Debye lengths *D*. The threshold energies $E_T$ are associated with the excited *nd* states of the parent (H or Ps) atom. The notation A(−B) denotes. A × $10^{-B}$. Units are in a.u.

| | *D* | $E_r$ (a.u.) | Γ/2 (a.u.) | $E_T$ | H or Ps State |
|---|---|---|---|---|---|
| H(3d°-1) | ∞ | −0.0555696 | 6.5795(−6) | −0.0555555 | H(3d) |
| | ∞ | −0.05557 [a] | 5.0(−7) [a] | | |
| | ∞ | −0.05558 [b] | 4.46(−6) [b] | | |
| | 400 | −0.053096 | 6.5869(−6) | −0.0530880 | |
| | 200 | −0.050681 | 6.7693(−6) | −0.0506843 | |
| | 133 | −0.0483112 | 7.1902(−6) | −0.0483252 | |
| | 100 | −0.0460441 | 7.8265(−6) | −0.0460614 | |
| | 80 | −0.0438323 | 8.6915(−6) | −0.0438393 | |
| H(4d°-1) | ∞ | −0.03491874 | 1.4823 (−5) | −0.03125 | H(4d) |
| | ∞ | −0.03492 [a] | 1.5(−5) [a] | | |
| | ∞ | −0.03487 [b] | 1.52(−5) [b] | | |
| | 200 | −0.0300559 | 1.4717(−5) | −0.0265028 | |
| | 100 | −0.0233321 | 1.3897(−5) | −0.0222277 | |
| | 50 | −0.0173629 | 1.2121(−5) | −0.0149400 | |
| | 40 | −0.0138259 | 1.0457(−5) | −0.0118704 | |
| | 30 | −0.0087534 | 7.4452(−6) | −0.0075337 | |
| H(4d°-2) | ∞ | −0.03189629 | 5.1879(−6) | −0.03125 | H(4d) |
| | ∞ | −0.03190 [a] | 5.0(−6) [a] | | |
| | ∞ | −0.03187 [b] | 5.5(−6) [b] | | |
| | 200 | −0.0270512 | 5.0904(−6) | −0.0265028 | |
| | 100 | −0.0225821 | 4.4915(−6) | −0.0222277 | |
| | 80 | −0.0205107 | 4.2532(−6) | −0.0202541 | |
| H(4d°-3) | ∞ | −0.0316152 | 1.0755(−5) | −0.03125 | H(4d) |
| | ∞ | −0.03162 [a] | 1.1(−5) [a] | | |
| | ∞ | −0.03157 [b] | 1.09(−5) [b] | | |
| | 200 | −0.0268033 | 1.0556(−5) | −0.0265028 | |
| | 100 | −0.0223763 | 9.6732(−6) | −0.0222277 | |
| | 80 | −0.0203119 | 8.9832(−6) | −0.0202541 | |
| H(4d°-4) | ∞ | −0.0313742 | 3.9334(−5) | −0.03125 | H(4d) |
| | ∞ | −0.03138 [a] | 2.5(−6) [a] | | |
| | ∞ | −0.03134 [b] | 1.29(−5) [b] | | |
| | 200 | −0.0265396 | 4.4088(−5) | −0.0265028 | |
| | 100 | −0.0221649 | 6.8085(−5) | −0.0222277 | |
| | 80 | −0.0201687 | 8.7066(−5) | −0.0202541 | |
| | 70 | −0.0188192 | 1.0138(−4) | −0.0189080 | |

[a] Ref. [9]; [b] Ref. [13].

## 4. Conclusions

In the present work, we report results of resonance parameters (energy and width) for the *P*-wave (with unnatural parity) and *D*-wave (with both natural and unnatural parities) in the positron-hydrogen system interacting with screened Coulomb potentials. By employing highly correlated Hylleraas functions and using the complex-scaling method for resonance calculations, some lower-lying resonance states in the said system up to the H($N$ = 4) threshold are determined under various screening strength conditions, and the behaviors for such resonance states in the case of screened Coulomb potential are also discussed. It is hoped that our findings will provide useful references to the communities in atomic physics, positron physics, plasma physics, and nuclear physics, as our method can also be applied to systems with Yukawa potentials. In addition, it is hoped that our work will stimulate further investigations on resonances with screened Coulomb potentials, or other forms of screening potentials such as the exponential cosine screened Coulomb potentials, on systems with positron-atom interactions. Finally, we should mention that at present it is unlikely that there will be any experimental confirmation of our present results. However, we are confident that our results are quite accurate and hope that they would provide motivation to experimentalists to search for such resonances in positron-hydrogen scattering, with and without the screened Coulomb effect.

**Acknowledgments:** Ye Ning and Zong-Chao Yan were supported by Natural Sciences and Engineering Research Council of Canada, the Atlantic Computational Excellence Network, and the Shared Hierarchical Academic Research Computing Network of Canada. Yew Kam Ho was supported by Ministry of Science and Technology of Taiwan.

**Author Contributions:** All authors have made contributions leading to the results presented in the present work. All authors have read and approved the final version of manuscript.

**Conflicts of Interest:** The authors declare no conflict of interest.

## References

1. Mittleman, M.H. Resonances in proton-hydrogen and positron-hydrogen scattering. *Phys. Rev.* **1966**, *152*, 76. [CrossRef]
2. Doolen, G.D.; Nuttall, J.; Wherry, C.J. Evidence for a resonance in $e^+$-H *S*-wave scattering. *Phys. Rev. Lett.* **1978**, *40*, 313. [CrossRef]
3. Ho, Y.K.; Greene, C.H. On the positron-hydrogen resonances associated with the $N$ = 2 positronium and $N$ = 3 hydrogen thresholds. *Phys. Rev. A* **1987**, *35*, 3169–3171. [CrossRef] [PubMed]
4. Ho, Y.K. Positron-hydrogen resonances associated with the $N$ = 3 positronium and $N$ = 4 hydrogen thresholds. *Phys. Rev. A* **1988**, *38*, 6424–6425. [CrossRef] [PubMed]
5. Bhatia, A.K.; Drachman, R.J. Search for resonances in positron-atom systems. *Phys. Rev. A* **1990**, *42*, 5117. [CrossRef] [PubMed]
6. Ho, Y.K. *P*-wave resonances in positron-hydrogen scattering. *J. Phys. B* **1990**, *23*, L419–L422. [CrossRef]
7. Yan, Z.C.; Ho, Y.K. *D*-wave resonances in $e^+$-H scattering. *J. Phys. B At. Mol. Phys.* **2002**, *35*, 1875. [CrossRef]
8. Ho, Y.K.; Yan, Z.C. High partial wave resonances in positron hydrogen scattering. *Phys. Rev. A* **2004**, *70*, 032716. [CrossRef]
9. Yan, Z.C.; Ho, Y.K. Resonances with unnatural parities in the positron-hydrogen system. *Phys. Rev. A* **2008**, *77*, 030701. [CrossRef]
10. Shimamura, I.; Wakimoto, H.; Igarashi, A. Resonance states of unnatural parity in positronic atoms. *Phys. Rev. A* **2009**, *80*, 032708. [CrossRef]
11. Ma, J.; Zhou, Y.J.; Wang, Y.C. Unnatural parity resonance states in positron-excited hydrogen scattering. *Chin. Phys. B* **2012**, *21*, 123403. [CrossRef]
12. Yu, R.M.; Cheng, Y.J.; Jiao, L.G.; Zhou, Y.J. Resonances in positron hydrogen scattering above the H ($n$ = 2) Threshold. *Chin. Phys. Lett.* **2012**, *29*, 053401. [CrossRef]
13. Umair, M.; Jonsel, S. Natural and unnatural parity resonance states in positron–hydrogen scattering. *J. Phys. B At. Mol. Opt. Phys.* **2014**, *47*, 225001. [CrossRef]
14. Ho, Y.K.; Yan, Z.C. High-angular momentum resonances in $e^+$-$He^+$ scattering. *Phys. Rev. A* **2002**, *66*, 062705. [CrossRef]

15. Roy, U.; Ho, Y.K. *S*-wave resonances in positron-lithium scattering. *J. Phys. B* **2002**, *35*, 1875–1883. [CrossRef]
16. Roy, U.; Ho, Y.K. *P*-wave resonances in $e^+$-Li scattering. *Nucl. Instrum. Methods B* **2004**, *221*, 36–40. [CrossRef]
17. Kar, S.; Ho, Y.K. *S*-wave resonances in $e^+$-He scattering below the Ps ($n = 2$) excitation threshold. *J. Phys. B* **2004**, *37*, 3177–3186. [CrossRef]
18. Kar, S.; Ho, Y.K. *S*-wave resonances in positron scattering from Na and K. *Eur. Phys. J. D* **2005**, *35*, 453. [CrossRef]
19. Han, H.L.; Zhong, Z.X.; Zhang, X.Z.; Shi, T.Y. *S*-wave resonances in positron-lithium scattering below the Li ($n = 4$) thresholds. *Phys. Rev. A* **2008**, *78*, 044701. [CrossRef]
20. Umair, M.; Jonsell, S. Resonances with natural and unnatural parities in positron-sodium scattering. *Phys. Rev. A* **2015**, *92*, 012706. [CrossRef]
21. Ren, Z.Z.; Han, H.L.; Shi, T.Y. *S*-wave resonances in the positron–helium scattering. *J. Phys. B At. Mol. Opt. Phys.* **2011**, *44*, 065204. [CrossRef]
22. Ho, Y.K. The method of complex coordinate rotation and its applications to atomic collision processes. *Phys. Rep.* **1983**, *99*, 1. [CrossRef]
23. Ho, Y.K. Resonances in positron-atom scattering. *Hyperfine Interact.* **1992**, *73*, 109–130.
24. Ho, Y.K. Resonances in three-body atomic systems involving positrons. *Chin. J. Phys.* **1997**, *35*, 97.
25. Ho, Y.K. Atomic resonances involving positrons. *Nucl. Instrum. Methods Phys. Res. B* **2008**, *266*, 516–521. [CrossRef]
26. Ho, Y.K. Recent Advances in the theoretical methods and computational schemes for Investigations of resonances in few-body atomic systems. *Few-Body Syst.* **2013**, *54*, 31–37. [CrossRef]
27. Debye, P.; Hückel, E. The theory of electrolytes. I. Lowering of freezing point and related phenomena. *Phys. Z.* **1923**, *24*, 185–206.
28. Salzman, D. *Atomic Physics in Hot Plasmas*; Oxford University Press: Oxford, UK, 1998.
29. Ichimarn, S. Strongly coupled plasmas: High-density classical plasmas and degenerate electron liquids. *Rev. Mod. Phys.* **1982**, *54*, 1017. [CrossRef]
30. Sil, A.N.; Canuto, S.; Mukherjee, P.K. Spectroscopy of confined atomic systems: Effect of plasma. *Adv. Quantum Chem.* **2009**, *58*, 115.
31. Paul, S.; Ho, Y.K. Combined effect of Debye plasma environment and external electric field on hydrogen atom. *Phys. Plasmas* **2010**, *17*, 082704. [CrossRef]
32. Lin, Y.C.; Lin, C.Y.; Ho, Y.K. Spectral data of helium atoms with screened Coulomb potentials using the *B*-spline approach. *Phys. Rev. A* **2012**, *85*, 042516. [CrossRef]
33. Pandey, M.K.; Lin, Y.C.; Ho, Y.K. Investigation of charge transfer and ionization in He-like systems ($Li^+$, $Be^{2+}$, $B^{3+}$, $C^{4+}$, $N^{5+}$, $O^{6+}$)-hydrogen atom collisions in Debye plasmas. *Phys. Plasmas* **2013**, *20*, 022104. [CrossRef]
34. Chang, T.N.; Fang, T.K.; Ho, Y.K. One- and two-photon ionization of hydrogen atom embedded in Debye plasmas. *Phys. Plasmas* **2013**, *20*, 092110. [CrossRef]
35. Lin, Y.C.; Fang, T.K.; Ho, Y.K. Quantum entanglement for helium atom in the Debye plasmas. *Phys. Plasmas* **2015**, *22*, 032113.
36. Pandey, M.K.; Lin, Y.C.; Ho, Y.K. An investigation of antiprotons collisions with positronium atom in Debye plasma environments. *Phys. Plasmas* **2015**, *22*, 052104. [CrossRef]
37. Kar, S.; Ho, Y.K. Autoionizing $^1S^e$ resonance of $H^-$ in Debye plasma environments. *Phys. Rev. E* **2004**, *70*, 066411. [CrossRef] [PubMed]
38. Chakraborty, S.; Ho, Y.K. Complex-scaling treatment for high-lying doubly excited resonances for screened Coulomb helium atom. *Eur. Phys. J. D* **2008**, *49*, 59–65. [CrossRef]
39. Ghoshal, A.; Ho, Y.K. Doubly excited resonance states of helium in exponential cosine-screened Coulomb potentials. *Phys. Rev. A* **2009**, *79*, 062514. [CrossRef]
40. Jiao, L.G.; Ho, Y.K. Shape resonances in the electron-hydrogen system with screened Coulomb potentials. *Phys. Rev. A* **2013**, *87*, 052508. [CrossRef]
41. Jiao, L.G.; Ho, Y.K. Doubly excited *P*-wave resonance states of $H^-$ in Debye plasmas. *Phys. Plasmas* **2013**, *20*, 083303. [CrossRef]
42. Jiao, L.G.; Ho, Y.K. Doubly-excited $2p^2\,{}^3P^e$ state of the hydrogen negative ion in Debye plasmas. *J. Quant. Spectrosc. Radiat. Transf.* **2014**, *144*, 27–35. [CrossRef]
43. Jiang, P.; Kar, S.; Zhou, Y. Doubly excited states of the hydrogen negative ion and helium in astrophysical plasmas. *Phys. Plasmas* **2013**, *20*, 012126. [CrossRef]

44. Rej, P.; Ghoshal, A. Positron impact excitations of hydrogen atom embedded in weakly coupled plasmas: Formation of Rydberg atoms. *Phys. Plasmas* **2014**, *21*, 093507. [CrossRef]
45. Bhattacharya, A.; Kamali, M.Z.M.; Ghoshal1, A.; Ratnavelu, K. Positron scattering from hydrogen atom embedded in dense quantum plasma. *Phys. Plasmas* **2013**, *20*, 083514. [CrossRef]
46. Ma, J.; Cheng, Y.; Wang, Y.C.; Zhou, Y. Positronium formation in positron-hydrogen collisions with Debye potentials. *Phys. Plasmas* **2012**, *19*, 063303. [CrossRef]
47. Kar, S.; Ho, Y.K. S-wave resonances in the positron–hydrogen system with screened Coulomb potentials. *J. Phys. B* **2005**, *38*, 3299. [CrossRef]
48. Chakraborty, S.; Ho, Y.K. Determination of resonance parameters for the $e^+$-H system in Debye plasma environments using the complex-coordinate-rotation method. *Phys. Rev. A* **2008**, *77*, 014502. [CrossRef]
49. Ning, Y.; Yan, Z.C.; Ho, Y.K. An investigation of resonances in $e^+$-H scattering embedded in Debye plasm. *Phys. Plasmas* **2015**, *22*, 013302. [CrossRef]
50. Jiang, Z.S.; Zhang, Y.Z.; Kar, S. Resonances in positron-hydrogen scattering in dense quantum plasmas. *Phys. Plasmas* **2015**, *22*, 052105. [CrossRef]
51. Yan, Z.C.; Drake, G.W.F. On the evaluation of 2-electron integrals in Hylleraas coordinates. *Chem. Phys. Lett.* **1996**, *259*, 96. [CrossRef]